Solar Phys (2012) 278:121–136
DOI 10.1007/s11207-011-9923-2

Velocity Characteristics of Rotating Sunspots

C. Zhu · D. Alexander · L. Tian

Received: 2 May 2011 / Accepted: 8 December 2011 / Published online: 11 January 2012

Abstract A statistical study is carried out to investigate the detailed relationship between rotating sunspots and the emergence of magnetic flux tubes. This paper presents the velocity characteristics of 132 sunspots in 95 solar active regions. The rotational characteristics of the sunspots are calculated from successive SOHO/MDI magnetograms by applying the Differential Affine Velocity Estimator (DAVE) technique (Schuck, 2006, *Astrophys. J.* **646**, 1358). Among 82 sunspots in active regions exhibiting strong flux emergence, 63 showed rotation with rotational angular velocity larger than 0.4° h^{-1}. Among 50 sunspots in active regions without well-defined flux emergence, 14 showed rotation, and the rotation velocities tend to be slower, compared to those in emerging regions. In addition, we investigated 11 rotating sunspot groups in which both polarities show evidence for co-temporary rotation. In seven of these cases the two polarities co-rotate, while the other four are found to be counter-rotating. Plausible reasons for the observed characteristics of the rotating sunspots are discussed.

Keywords Flares, relation to magnetic field · Sunspots, velocity

1. Introduction

Sunspots are frequently observed to exhibit a prolonged period of rotation about their center (*e.g.*, Evershed, 1909; Nightingale *et al.*, 2001). Brown *et al.* (2003) studied seven rotating sunspots and revealed that some rotated up to a total of 200° around their center over a period of three to five days.

Flux Emergence in the Hinode Era
Guest Editor: L.M. Green

C. Zhu · D. Alexander (✉) · L. Tian
Department of Physics and Astronomy, Rice University, 6100 Main, Houston, TX, USA
e-mail: dalex@rice.edu

C. Zhu
e-mail: cz3@rice.edu

Sunspot rotation can contribute significantly to the magnetic helicity injection into the solar corona, causing a non-potential coronal magnetic field, which is generally believed to be the energy source for solar flares and CMEs (Rust and Kumar, 1994; Low, 1996; Canfield, Hudson, and McKenzie, 1999; Pevtsov, 2002; Kazachenko *et al.*, 2009). Zhang, Liu, and Zhang (2008) studied the rotating sunspot in AR 10486, and suggested that the rotational motions of sunspots not only transport magnetic energy and complexity from the low atmosphere to the corona but may also play an important role in the onset of the observed homologous flares. Yan, Qu, and Xu (2008) performed a statistical study on the relationship between rotating sunspots and flare productivity, revealing that the rotational motions can contribute to the energy buildup in solar flares.

Several mechanisms have been introduced to explain the observed sunspot rotation. One obvious possibility would be the presence of rotating structures in the photospheric flow field (see discussions in Brown *et al.* (2003)). An alternative possibility would be that the observed rotation is an artifact of the emergence of a twisted flux tube with two possible scenarios having been proposed: one states that the apparent rotation is a result of the projected velocity of a twisted flux tube rising through the photosphere (Démoulin and Berger, 2003); the other states that the flux-tube would be expected to spin about its axis, resulting from a net axial torque caused by an unbalanced twist density across the photospheric layer (Longcope and Welsch, 2000). Simulations (Magara and Longcope, 2003; Gibson *et al.*, 2004; Fan, 2009) typically show that rotating sunspots are prevalent during the emergence of a twisted flux tube (Ω-loop). Brown *et al.* (2003) pointed out that flux-tube emergence would be one important mechanism leading to rotating sunspots, but they also pointed out that further analysis was needed to determine the primary mechanism responsible for the observed rotation. Recently, Min and Chae (2009) found that the characteristics and behavior of a rotating sunspot in AR 10930 support the idea that the rotation of the sunspot may have been driven by the emergence of a pre-twisted flux tube.

The detailed relationship between the emergence of a twisted flux tube and sunspot rotation still remains unclear, and the answer to this question would help us get a better understanding of the primary mechanisms driving flux emergence and the impact this has on the photosphere and corona. In this paper, we present a statistical study of the relationship between the rotation velocity of sunspots and magnetic flux emergence in a large number of solar active regions. We also identify a number of cases of multiple rotating sunspots in the same active region. This paper is organized as follows: Section 2 introduces data and our method for determining sunspot rotating velocity with the Differential Affine Velocity Estimator (DAVE) method (Schuck, 2006). Section 3 discusses our statistical study on the relationship of sunspot rotation and flux tube emergence, with active regions containing multiple rotating sunspots considered in Section 4. We conclude with a discussion in Section 5.

2. Data and Method

In this study, we use line-of-sight magnetograms from SOHO/MDI (Scherrer *et al.*, 1995), with temporal resolution of 96 min and spatial resolution of about $2''$. There are 2727 active regions reported by the National Oceanic and Atmospheric Administration (NOAA) between December 1997 and December 2005. The distribution of the sizes of these active regions is shown in Figure 1 (ten active regions with size larger than 1500 millionths of a solar disk are not included in this figure). The criteria for selection of the active regions in the study reported here are as follows:

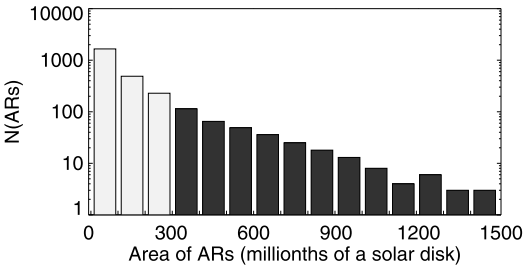

Figure 1 Size distributions of the active regions (ARs) from Dec. 1997 to Dec. 2005. Shaded columns indicate active regions with areas larger than 300 millionths of a solar disk.

i) The active region is larger than 300 millionths of a solar disk (shaded dark in Figure 1), which yields a higher probability of finding large sunspots.
ii) The active region is located near the center of the solar disk, in the region surrounded by ±40° EW and ±40° NS (*e.g.*, Chae and Jeong, 2005).
iii) There is no evidence for magnetic saturation in the MDI data, which mainly results from the low intensity in the umbra and the limitations of the MDI on-board algorithm (Liu, Norton, and Scherrer, 2007).

As a result, our study consists of a sample of 132 sunspots contained in 95 separate active regions.[1]

The MDI data for a given active region are derotated to remove the effect of solar differential rotation (Chae and Jeong, 2005). The flow field is calculated using the DAVE method (Schuck, 2006), which is a robust and accurate velocity inversion technique developed for use with line-of-sight magnetograms (Welsch *et al.*, 2007). It adopts an affine velocity profile and minimizes deviations in the magnitude of the magnetic induction equation within a windowed subregion of successive magnetograms. The magnetic-flux-weighted center of a sunspot (*e.g.*, Tian *et al.*, 2005) is determined by

$$x_{\mathrm{c}} = \frac{\sum x(i,j) B_{\mathrm{n}}(i,j)\,\mathrm{d}s}{\sum B_{\mathrm{n}}(i,j)\,\mathrm{d}s}, \qquad y_{\mathrm{c}} = \frac{\sum y(i,j) B_{\mathrm{n}}(i,j)\,\mathrm{d}s}{\sum B_{\mathrm{n}}(i,j)\,\mathrm{d}s} \tag{1}$$

where B_{n} is the normal component of the magnetic field (Chae *et al.*, 2001), $x(i,j)$ and $y(i,j)$ denotes the position of a pixel on the magnetogram with magnetic field strength of $B_{\mathrm{n}}(i,j)$, and ds is the subregion that the selected sunspot, or polarity, covers.

To determine the velocity, we chose a radial distance, r, from the flux-weighted center of the sunspot under consideration (see Figure 2). The sunspot rotation profile changes with respect to radius (Brown *et al.*, 2003), and is found to be slowest in the umbra and fastest in the penumbra. For clarity, in the present study we concentrate on the umbra-penumbra boundary, where the magnetic field has magnitude of about 1000 G (gauss) (Solanki, 2003). The angular velocity $\boldsymbol{\omega}$ of a sunspot at a distance r is

$$\boldsymbol{\omega} = \frac{1}{N} \sum_{i=1}^{N} \frac{\hat{\mathbf{r}} \times (\mathbf{v}_i - \bar{\mathbf{v}})}{r} \tag{2}$$

where $\bar{\mathbf{v}}$ is the flux-weighted velocity within the sunspot, and $\hat{\mathbf{r}}$ is a unit vector.

With this method, we compared four cases (ARs 9004, 9114, 9280, 10030) considered in the study of Brown *et al.* (2003). The other three cases are not used due to their position

[1] Within this sample, there are 11 sunspots which show an evolution from an emerging to a steady phase as time proceeds. Because of this, these sunspots appear in two different studies: the emergence study and the non-emergence study. But when they do, we restrict considerations to the relevant phase.

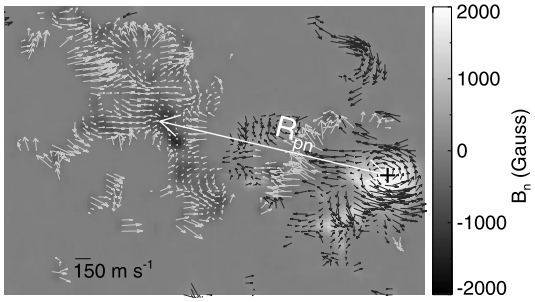

Figure 2 Map of velocity derived from the DAVE technique (see text) superposed on the gray-scale map of B_n from MDI line-of-sight magnetograms. The "+" sign denotes the center of the rotating sunspot. The dashed circle indicates the radius chosen to measure the angular velocity. "R_{pn}" denotes the footpoint separation of leading and following polarities.

Table 1 Comparison of rotations calculated with the DAVE method (θ_D) and rotations given in Brown *et al.* (2003) (θ_B).

	AR 9004	AR 9114	AR 9280	AR 10030
Date	19 – 21 May 2000	8 – 10 Aug. 2000	23 – 26 Dec. 2000	13 – 17 July 2002
Latitude	N15	N06	N12	N16
θ_B	90 – 120°	120 – 150°	50 – 130°	160 – 200°
θ_D	70°	120°	60°	160°

(AR 8668 and AR 9354) or small area (AR 9077). The result of this comparison is listed in Table 1. We find that the sunspot rotation calculated with the DAVE method (θ_D) is consistent with rotation reported in the study of Brown *et al.* (2003) (θ_B). The slight difference could come from the lower resolution of the MDI data we applied here and the data gap in the TRACE white-light data used in Brown *et al.* (2003) (*e.g.*, a gap of about 17 h exists in the study of AR 9004).

In order to determine whether each selected active region is emerging or not during the observational period, its total unsigned magnetic flux ϕ_{tot} and distance between the flux-weighted centers of the leading and following polarities (denoted by "R_{pn}") are calculated. From our sample of 132 sunspots, we find 82 associated with emerging active regions (*i.e.*, ϕ_{tot} and R_{pn} are increasing with time), and 50 are related to active regions in a post-emergence phase (*i.e.*, ϕ_{tot} and R_{pn} maintain at a steady value or decay). We provide a quantitative description of specific examples of the kinds of behavior observed in this sample of rotating sunspots in the following sections.

3. Observations

We break the discussion of our observations into the two categories: emerging and non-emerging active regions.

3.1. Rotation of Sunspots during the Emergence of Active Regions

In this subsection, we focus on the characteristics of the rotating sunspots from our sample in active regions that exhibit clear evidence for ongoing flux emergence. AR 9563 and AR 10226 are detailed as examples.

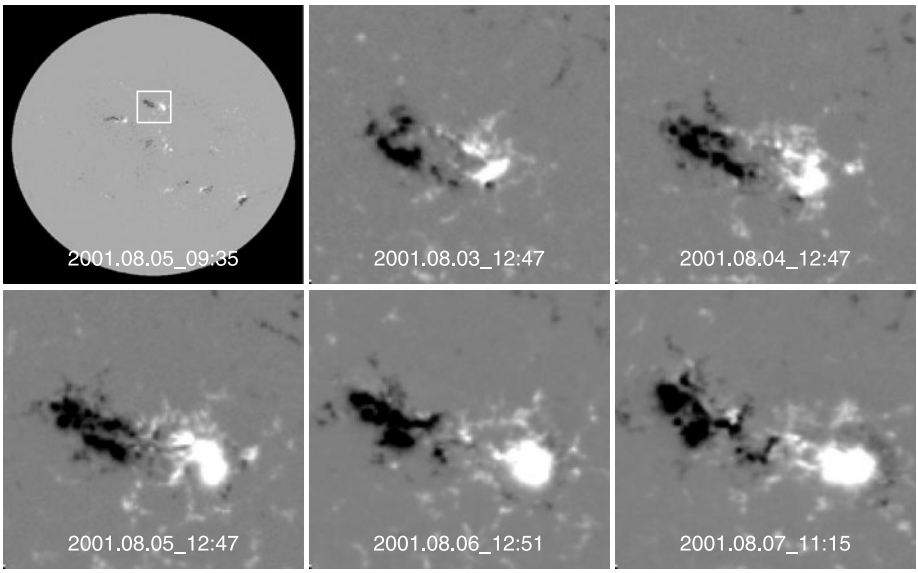

Figure 3 SOHO/MDI line-of-sight magnetograms of AR 9563. Its position on the solar disk is shown in the square box (top left panel).

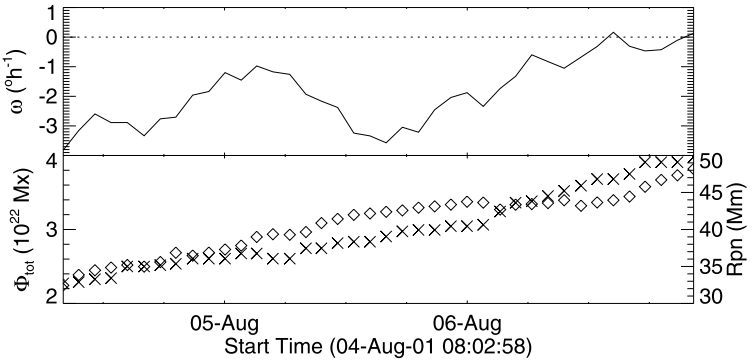

Figure 4 Angular velocity profile (ω, solid line) of the leading sunspot in AR 9563. The increasing total unsigned magnetic flux ($\phi_{\rm tot}$, "◇") and footpoint separation ($R_{\rm pn}$, "×") indicates this is an emerging active region.

AR 9563 was observed in the northern hemisphere from 2 to 14 August 2001, lying 20° from the equator. Figure 3 displays SOHO/MDI magnetograms of AR 9563. From 4 to 6 August, the leading sunspot in AR 9563 was observed to rotate clockwise through a total angle of about 120°. It is important to note that, as the observations usually do not cover the full time development of the active regions from initial emergence, the measured total rotations quoted are expected to be under-estimates in most cases.

Figure 4 shows the rotation speed of the leading sunspot of AR 9563, denoted by the solid line. During the three-day set of observations, the total unsigned magnetic flux $\phi_{\rm tot}$ increased gradually from 2.1×10^{22} Mx (maxwell) to 3.8×10^{22} Mx, and the footpoint separation distance $R_{\rm pn}$ from 34 Mm to 51 Mm, indicating that AR 9563 is emerging during

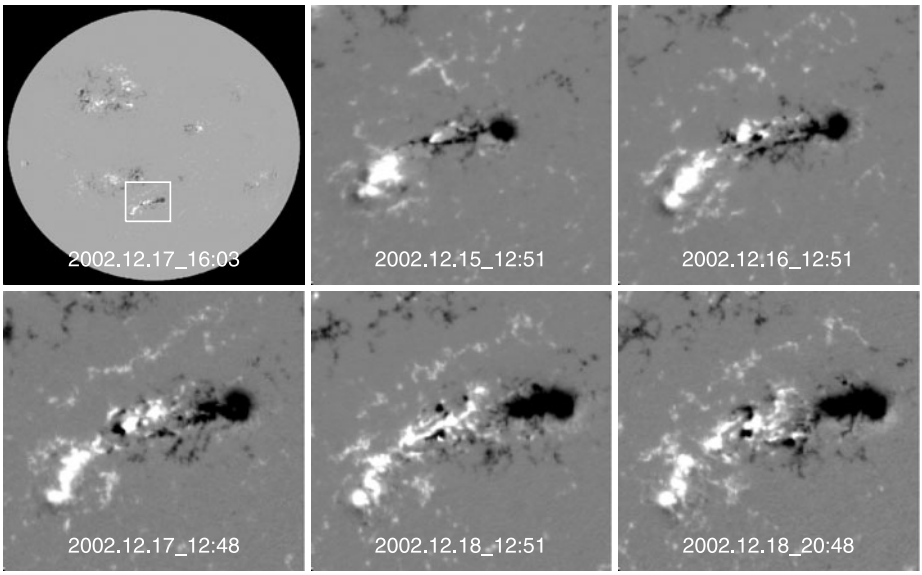

Figure 5 SOHO/MDI line-of-sight magnetograms of AR 10226.

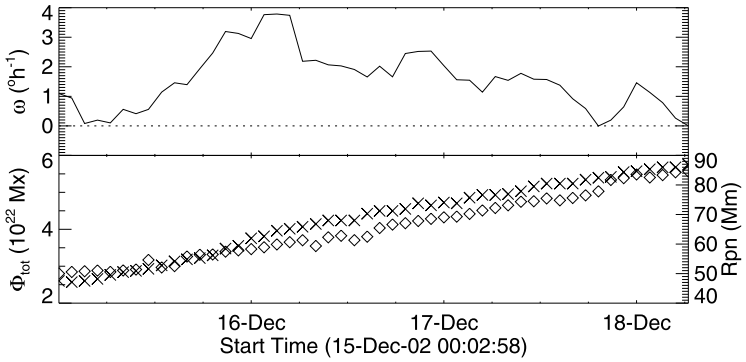

Figure 6 Angular velocity profile (ω, solid line) of the leading sunspot in AR 10226. The increasing total unsigned magnetic flux ($\phi_{\rm tot}$, "◇") and footpoint separation ($R_{\rm pn}$, "×") indicates this is an emerging active region.

this period. The average angular velocity of the leading sunspot is about 1.8° h^{-1}, with a peak value of 3.7° h^{-1}. Moreover, the direction of its rotation remains clockwise throughout the observational period.

The leading sunspot in AR 10226 is another example of sunspot rotation occurring during the emergence phase of the active region. This active region was located in the southern hemisphere, with a latitude of about 25° S. Its evolution is shown in Figure 5. During the period of 80 h after 00:02 UT on 15 December 2002, it rotated in a counter-clockwise direction, through a total angle of 120°. Figure 6 shows the relationship between the time variation of the angular rotation speed and that of the flux tube emergence for this active region. The separation between the two polarities increased from 45 Mm to 86 Mm, while the

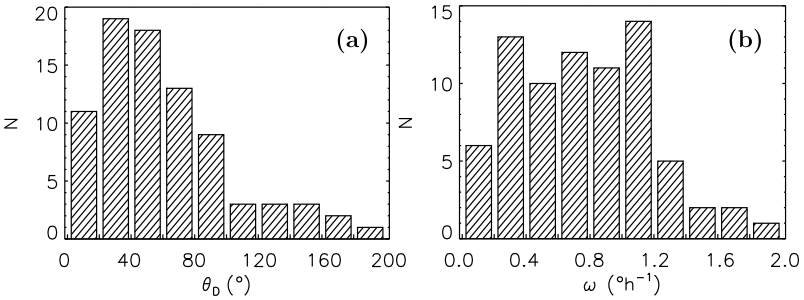

Figure 7 Total rotation angle (left) and angular velocity (right) distributions of 82 rotating sunspots associated with the emergence of active regions.

total unsigned magnetic flux from 2.5×10^{22} Mx to 5.3×10^{22} Mx, indicating an emerging active region. The leading sunspot showed strong counter-clockwise rotation with an average value of 1.5° h^{-1} and a peak value of 3.8° h^{-1} during 16 December 2002. The rotation speed then gradually slowed down until it stopped rotating at the end of the observation period. The following polarity became significantly dispersed after 17 December 2002, and no evident rotation was found in this polarity.

From our total sample, there are 82 sunspots identified to be associated with emerging active regions (Table 2). Figure 7a shows the distribution of the rotational parameters for all 82 sunspots. The most pronounced rotation was detected in AR 9114, which had a total counter-clockwise rotation angle of about 180° over five days. Among these 82 sunspots, 63 are found to be in rotation with an average velocity, at the umbra/penumbra boundary, greater than 0.4° h^{-1}, as seen in Figure 7b, while the remaining 19 sunspots do not show well-defined rotation, exhibiting angular velocities $\omega \lesssim 0.4°$ h^{-1} and/or frequent changes in the direction of rotation.

3.2. Rotation of Sunspots in the Post-Emergence Phase of Active Regions

Among our selected sunspots, there are 50 in active regions without growth of total unsigned flux or their polarity separation during the observation. In this subsection, the velocity characteristics of these sunspots are investigated.

AR 9289 was located in the southern hemisphere with a latitude of 5° S (see Figure 8). From 31 December 2000 to 3 January 2001, its leading sunspot was seen to rotate about 50° clockwise. The rotation profile is shown in Figure 9. During this period, the total unsigned magnetic flux showed a slight decrease, from 5.8×10^{22} Mx to 5.2×10^{22} Mx. The separation distance of the two polarity centers, $R_{\rm pn}$, was almost steady, staying at around 54 Mm. Both indicate AR 9289 was a post-emergence active region. The leading spot mainly rotated clockwise, with an average speed of 0.56° h^{-1} and a peak value of about 1.5° h^{-1}. These kinds of sunspot are classified as rotating sunspots in the post-emergence phase of active regions.

Figure 10 gives the distribution of the total rotation angles (Figure 10a) and average angular velocities (Figure 10b) of the 50 sunspots in our sample of post-emergence active regions (Table 3). Ten of these sunspots have total rotation angles larger than 40° and 14 rotate with an average velocity $\omega \gtrsim 0.4°$ h^{-1}. Compared to Figure 7, it is evident that, statistically, after the emergence of the active region has ceased, the sunspots tend to rotate more slowly than is typically seen during flux emergence.

Table 2 Rotation of sunspots during the emergence of active regions. L and F indicate leading and following polarities in an active region. θ_D and $\bar{\omega}$ mean the total rotation angle and average angular velocity, respectively.

AR	Start (UT)	Duration (h)	θ_D (°)	$\bar{\omega}$ (° h^{-1})
8156	02/14/1998 00:00	120	90	0.8
8214	05/01/1998 00:00	112	−90	−0.8
8404(L)	12/07/1998 20:00	40	50	1.3
8404(F)	12/07/1998 20:00	40	60	1.5
8562	06/01/1999 00:00	103	10	0.1
8574(L)	06/07/1999 17:36	69	−80	−1.2
8574(F)	06/07/1999 17:36	69	50	0.7
8611	06/30/1999 00:00	116	170	1.5
8614	07/04/1999 23:59	156	−10	0.0
8651(L)	07/31/1999 00:00	94	−90	−1.0
8651(F)	07/31/1999 00:00	94	40	0.4
8760	11/10/1999 00:00	66	10	0.2
8936	04/02/2000 00:00	115	40	0.4
8989	05/09/2000 23:59	69	−40	−0.6
8990	05/09/2000 23:59	117	90	0.8
8998	05/18/2000 14:24	31	10	0.3
9004(L)	05/19/2000 17:36	52	40	0.8
9004(F)	05/19/2000 17:36	52	−70	−1.4
9069(L)	07/09/2000 06:24	37	−40	−1.1
9069(F)	07/09/2000 06:24	37	−40	−1.1
9070(L)	07/08/2000 12:48	54	−50	−0.9
9070(F)	07/08/2000 12:48	54	−50	−0.9
9114	08/05/2000 23:59	116	185	1.6
9173(L)	09/27/2000 23:59	60	−100	−1.7
9173(F)	09/27/2000 23:59	60	−50	−0.8
9231	11/16/2000 23:59	91	110	1.2
9368(L)	03/03/2001 23:59	118	40	0.3
9368(F)	03/03/2001 23:59	118	90	0.8
9563	08/04/2001 08:03	67	−120	−1.8
9574	08/11/2001 00:03	66	−70	−1.1
9616	09/15/2001 23:59	93	60	0.7
9622	09/19/2001 23:59	45	60	1.4
9670	10/19/2001 23:59	118	−70	−0.6
9678	10/24/2001 23:59	41	30	0.7
9692(L)	11/07/2001 19:11	44	50	1.0
9692(F)	11/07/2001 19:11	44	5	0.1
9748	12/23/2001 00:03	66	90	1.3
9767	01/03/2002 23:59	51	−40	−0.7
9800(L)	01/28/2002 00:00	96	30	0.3
9800(F)	01/28/2002 00:00	96	30	0.3
9885	03/30/2002 00:00	45	50	1.2
9887(L)	04/01/2002 00:00	116	40	0.4
9887(F)	04/01/2002 00:00	116	−20	−0.1
9906(L)	04/13/2002 08:00	83	−80	−1.0

Table 2 (*Continued*)

AR	Start (UT)	Duration (h)	θ_D (°)	$\bar{\omega}$ (° h^{-1})
9906(F)	04/13/2002 08:00	83	−70	−0.8
9912(L)	04/20/2002 09:35	59	−60	−1.0
9912(F)	04/20/2002 09:35	59	−50	−0.8
9961	05/23/2002 00:00	62	100	1.6
10036(L)	07/19/2002 23:59	85	−30	−0.3
10036(F)	07/19/2002 23:59	85	10	0.1
10050	07/26/2002 23:59	113	−70	−0.6
10087	08/25/2002 23:59	109	−30	−0.2
10103	09/09/2002 04:51	63	−50	−0.9
10119	09/16/2002 23:59	120	130	1.1
10137	10/01/2002 00:00	104	70	0.7
10139(L)	10/06/2002 14:27	40	−20	−0.4
10139(F)	10/06/2002 14:27	40	−50	−1.2
10226	12/15/2002 00:03	80	120	1.5
10230	12/20/2002 00:00	96	−80	−0.9
10242	01/07/2003 09:39	59	−70	−1.1
10290	02/20/2003 00:00	52	−40	−0.8
10319	03/26/2003 20:48	64	30	0.4
10323	03/29/2003 00:00	66	−60	−0.9
10344(L)	04/26/2003 01:39	91	70	0.8
10344(F)	04/26/2003 01:39	91	−70	−0.8
10349	04/29/2003 00:03	72	−60	−0.8
10365(L)	05/25/2003 16:00	67	−20	−0.3
10365(F)	05/25/2003 16:00	67	−60	−0.9
10410	07/16/2003 01:39	54	−30	−0.5
10421	08/02/2003 00:00	69	70	1.0
10564(L)	02/21/2004 23:59	38	10	0.3
10564(F)	02/21/2004 23:59	38	−20	−0.6
10609	05/14/2004 00:00	97	40	0.4
10656	08/07/2004 23:59	140	150	1.1
10687	10/24/2004 00:03	93	120	1.3
10696(L)	11/03/2004 02:58	92	80	0.9
10696(F)	11/03/2004 02:58	92	110	1.2
10779	06/16/2005 00:03	48	20	0.4
10783	07/01/2005 23:59	93	40	0.5
10798(L)	08/18/2005 20:47	44	−40	−0.9
10798(F)	08/18/2005 20:47	44	40	0.9
10826	12/01/2005 00:00	58	40	0.6

In this section, we investigated 132 sunspots to explore the relationship between the rotating sunspots and the emergence of the active regions. Among 82 sunspots in emerging active regions, about 63 showed rotation with $\omega \gtrsim 0.4°$ h^{-1}, while the remaining sunspots do not show well-defined rotation. Among 50 sunspots in post-emergence active regions, only 14 are found to rotate with an average velocity larger than $0.4°$ h^{-1}. This indicates that

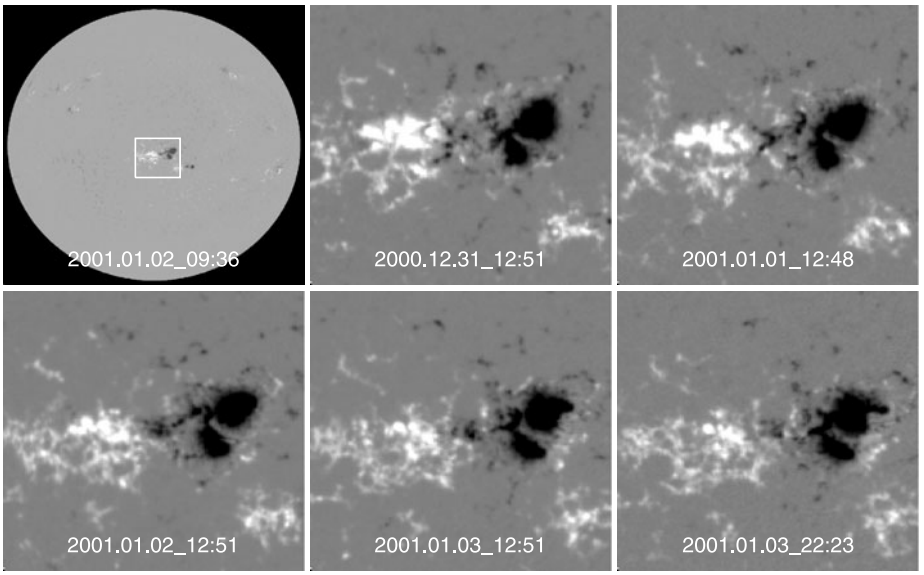

Figure 8 SOHO/MDI line-of-sight magnetograms of AR 9289.

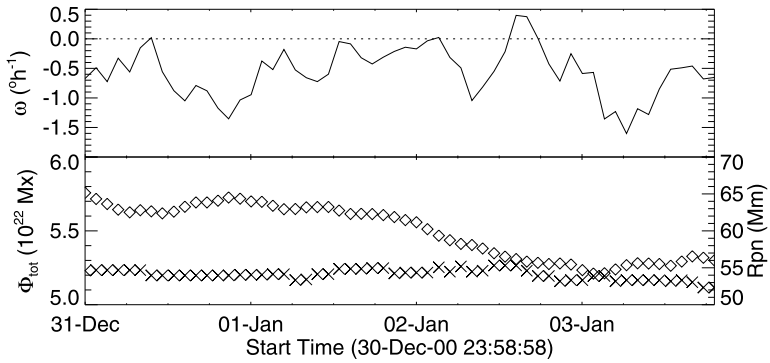

Figure 9 Angular velocity profile (ω, solid line) of the leading sunspot in AR 9289. The slightly decreasing total unsigned magnetic flux ($\phi_{\rm tot}$, "◇") and steady footpoint separation ($R_{\rm pn}$, "×") indicate this is a post-emergence active region.

rotating sunspots are strongly associated with the process of flux tube emergence, confirming previous expectations (Longcope and Welsch, 2000; Brown *et al.*, 2003; Min and Chae, 2009).

4. Rotating Sunspots in a Single Active Region

Occasionally, sunspots of both polarities in an active region are observed to rotate (Yan, Qu, and Xu, 2008); some rotate in the same direction (described as co-rotating sunspots here), others rotate in opposite directions (counter-rotating sunspots). This section describes some observations of both types of multiple rotating sunspots in the same active region.

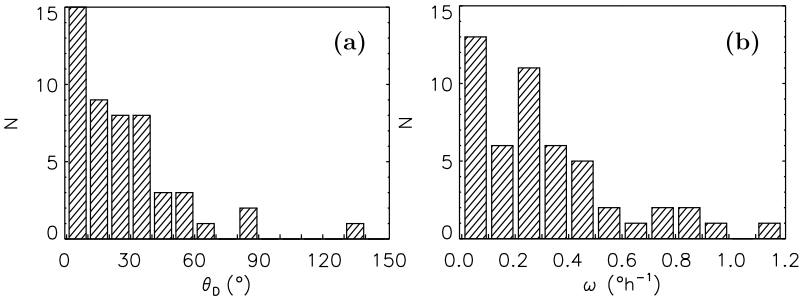

Figure 10 Total rotation angle (left) and angular velocity distributions (right) of post-emergence sunspots.

Table 3 Rotation of sunspots after the emergence of active regions.

AR	Start (UT)	Duration (h)	θ_D (°)	$\bar{\omega}$ (° h^{-1})
8558	06/01/1999 00:00	116	0	0.0
8739	10/23/1999 23:59	96	10	0.1
8742	10/27/1999 23:58	92	−40	−0.4
8882	02/24/2000 23:59	119	−40	−0.3
8921	03/24/2000 00:00	114	50	0.4
8955(L)	04/14/2000 23:59	117	−60	−0.5
8955(F)	04/14/2000 23:59	117	−30	−0.2
8970	04/25/2000 00:00	115	−20	−0.2
8998	05/18/2000 14:24	49	0	0.0
9033	06/10/2000 00:00	93	−10	−0.1
9046	06/19/2000 00:00	113	−30	−0.3
9062	06/29/2000 00:00	94	10	0.2
9097(L)	07/22/2000 01:35	116	−20	−0.2
9097(F)	07/22/2000 01:35	116	40	0.3
9176	09/30/2000 23:59	90	0	0.0
9289	12/30/2000 23:59	89	−50	−0.6
9454	05/14/2001 00:00	104	10	0.1
9678	10/26/2001 17:00	75	10	0.1
9717	12/01/2001 23:59	94	0	0.0
9767	01/07/2002 03:00	46	−20	−0.4
9871(L)	03/17/2002 00:00	115	−140	−1.2
9871(F)	03/17/2002 00:00	115	0	0.0
9945	05/10/2002 23:59	94	−40	−0.4
9961	05/25/2002 14:00	54	50	1.0
9973	06/01/2002 00:00	117	−40	−0.3

The leading positive-polarity sunspot and following negative-polarity sunspot in AR 10696 (Figure 11) were both observed to rotate counter-clockwise during the period from 3 to 6 November 2004. This active region was located in the northern hemisphere with latitude of 9° N. Figure 12 displays the angular velocities of both sunspots in this active region. The leading polarity showed an average velocity of 0.9° h^{-1} and a total rotation angle of about 80°, while the following polarity showed an average velocity of 1.2° h^{-1} and total

Table 3 (*Continued*)

AR	Start (UT)	Duration (h)	θ_D (°)	$\bar{\omega}$ (° h^{-1})
10061	08/07/2002 23:59	96	20	0.2
10095(L)	09/02/2002 23:59	71	−60	−0.8
10095(F)	09/02/2002 23:59	71	0	0.0
10139(L)	10/09/2002 06:30	50	−10	−0.3
10139(F)	10/09/2002 06:30	50	−10	−0.2
10207	12/01/2002 00:00	117	−40	−0.4
10290	02/22/2003 04:00	60	−30	−0.4
10325	04/01/2003 00:00	127	10	0.1
10337	04/23/2003 00:03	119	−30	−0.3
10349	05/02/2003 00:03	48	10	0.2
10365(L)	05/28/2003 11:00	38	10	0.3
10365(F)	05/28/2003 11:00	38	30	0.9
10380	06/10/2003 23:59	91	10	0.1
10424(L)	08/04/2003 23:59	114	−10	−0.1
10424(F)	08/04/2003 23:59	114	30	0.3
10517	12/04/2003 00:03	109	10	0.1
10528	12/21/2003 23:59	92	−30	−0.3
10540	01/16/2004 23:59	117	80	0.7
10551	02/07/2004 23:59	43	0	0.0
10554	02/11/2004 23:59	83	0	0.0
10564	02/23/2004 15:00	20	0	0.0
10693(L)	10/31/2004 00:00	116	30	0.2
10693(F)	10/31/2004 00:00	116	10	0.1
10743	03/12/2005 23:59	34	10	0.2
10826	12/03/2005 10:00	30	20	0.8

rotation angle of about 110°. Both total unsigned magnetic flux and the separation distance between the two sunspots increased rapidly, indicating these were co-rotating sunspots in an emerging active region. This scenario, in which sunspots in the active region rotate in the same direction, is believed to be effective for magnetic helicity injection and the subsequent storage of magnetic energy in the corona (*e.g.* Yan, Qu, and Xu, 2008).

AR 8574 is an example of an active region in which the sunspots were observed to rotate in the opposite direction. Its evolution is shown in Figure 13. It is evident that this active region emerges quickly from 6 to 10 June 1999. Figure 14 gives the rotation profile of the two polarities in AR 8574. During 69 hours after 17:36 UT in 7 June 1999, the leading polarity rotated about 80° clockwise with average rotational velocity $\bar{\omega} = -1.2°\ \mathrm{h}^{-1}$, while the following one (dashed line) rotated about 50° counter-clockwise with $\bar{\omega} = 0.7°\ \mathrm{h}^{-1}$.

In our sample of 95 active regions, there are seven co-rotating sunspot groups and four counter-rotating sunspot groups, as listed in Table 4. The rotation of sunspots in a given active region can be significantly different, such as in AR 8651, where the leading-polarity sunspot rotated about twice as fast as the following one. The co-rotation of two sunspots in the emerging active region has a relatively simple explanation and is in fact expected from the straightforward emergence of a uniformly twisted flux tube (Longcope and Welsch, 2000; Gibson *et al.*, 2004; Fan, 2009). But the presence of counter-rotating sunspots is somewhat of a surprise given that they are expected to result from the emergence of a mono-

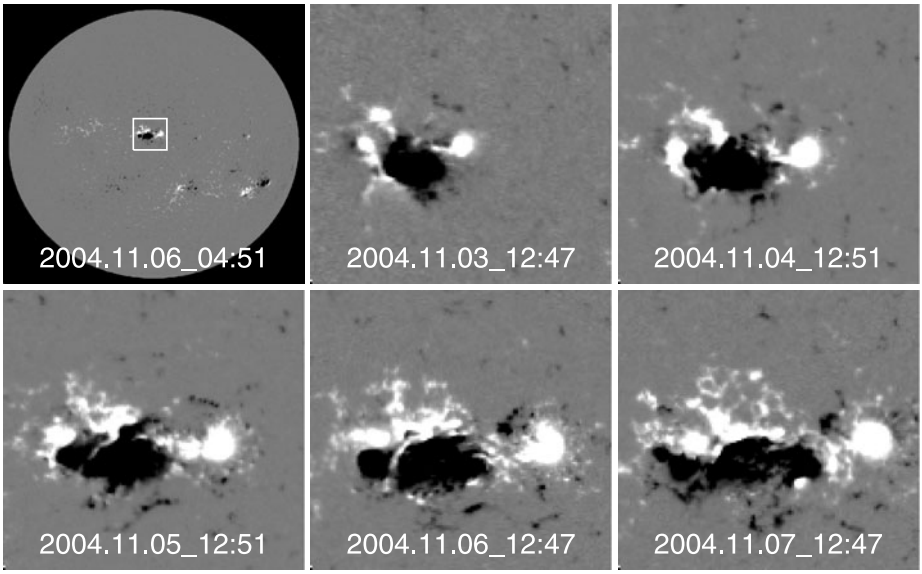

Figure 11 SOHO/MDI line-of-sight magnetograms of AR 10696.

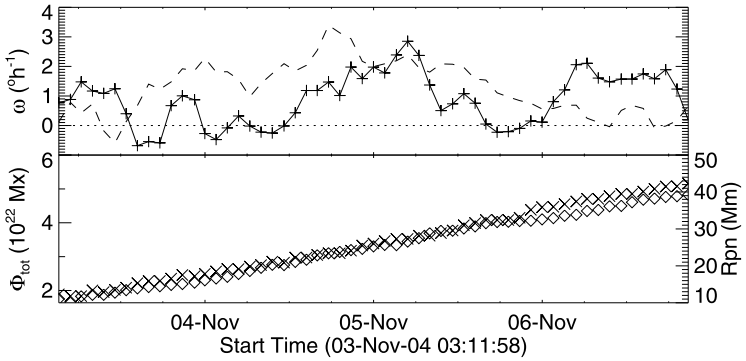

Figure 12 Multiple rotating sunspots in leading positive polarity (solid line with "+") and following negative polarity (dashed line) in AR 10696. The sign "◊" denotes total unsigned magnetic flux $\phi_{\rm tot}$, and "×" denotes footpoint separation of the two investigated sunspots.

lithic magnetic flux tube. This behavior is not captured by the currently available flux emergence simulations (Gibson *et al.*, 2004; Fan, 2009). A possible explanation for the observed counter-rotating sunspots is discussed in the last section.

5. Summary and Discussion

In order to determine the relationship between rotating sunspots and the emergence of magnetic flux tubes in solar active regions, 132 sunspots in 95 active regions were investigated. Among 82 sunspots in emerging active regions, 63 showed rotation with average angular velocity larger than 0.4° h^{-1}. When considering 50 sunspots without notable flux tube

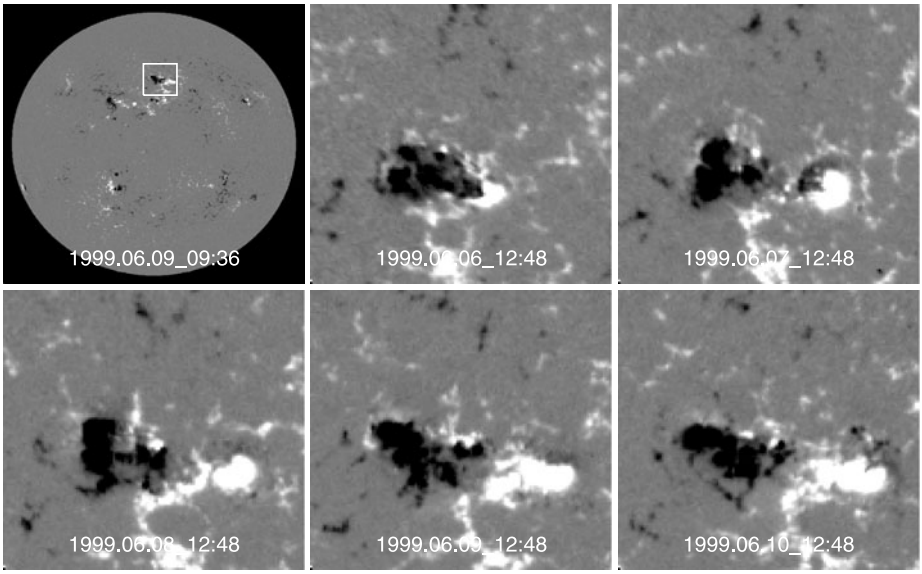

Figure 13 SOHO/MDI line-of-sight magnetograms of AR 8574.

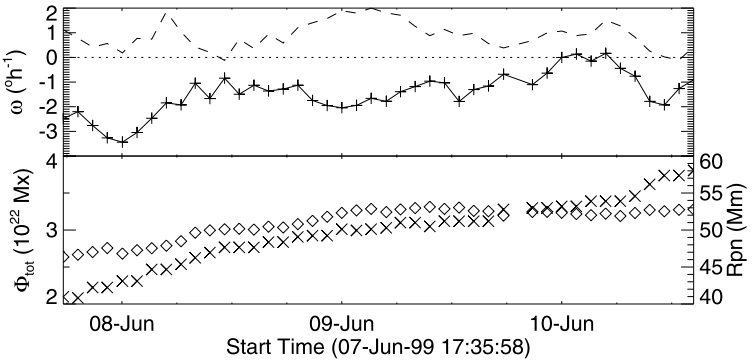

Figure 14 Multiple rotating sunspots in the leading positive polarity (solid line with "+") and following negative polarity (dashed line) in AR 8574. The sign "◊" denotes total unsigned magnetic flux $\phi_{\rm tot}$, and "×" denotes footpoint separation of the two investigated sunspots.

emergence, the rotation of these tend to stop early in the observation period or be relatively slow. This indicates that a strong relationship exists between sunspot rotation and flux emergence in active regions. Whether this observed relationship is a result of the emergence of a monolithic twisted flux tube or the generation of rotational surface flows driven by the emergence is still an outstanding question. Both mechanisms would imply a strong relationship between rotating sunspots and the emergence of active regions, as found in the analysis presented in this paper. However, an interesting phenomenon is that there are still about 14 of post-emergence sunspots with average rotating velocity larger than 0.4° h^{-1}. For these active regions without well-defined emergence, the projected velocity, if present, would be expected to be small, so the presence of rotating sunspots after the end of the emergence

Table 4 Rotating sunspot groups. θ_D and $\bar{\omega}$ mean the total rotation angle and average angular velocity, respectively.

AR	Start (UT)	Duration (h)	Leading polarity		Following polarity	
			θ_D (°)	$\bar{\omega}$ (° h^{-1})	θ_D (°)	$\bar{\omega}$ (° h^{-1})
8404	12/07/1998 20:00	40	50	1.3	60	1.5
9069	07/09/2000 06:24	37	−40	−1.1	−40	−1.1
9070	07/08/2000 12:48	54	−50	−0.9	−50	−0.9
9173	09/28/2000 00:00	60	−100	−1.7	−50	−0.8
9906	04/13/2002 08:00	83	−80	−1.0	−70	−0.8
9912	04/20/2002 09:35	59	−60	−1.0	−50	−0.8
10696	11/03/2004 02:58	92	80	0.9	110	1.2
8574	06/07/1999 17:36	69	−80	−1.2	50	0.7
8651	07/31/1999 00:00	94	−90	−1.0	40	0.4
9004	05/19/2000 17:36	52	40	0.8	−70	−1.4
10344	04/26/2003 01:39	91	70	0.8	−70	−0.8

suggests that the balance of the twist near the photosphere has not yet been reached, or is interrupted as a result of some other processes, such as solar flares (Y. Fan, private communication).

There are 11 active regions identified to contain multiple rotating sunspots. Seven show co-rotation, and the remaining four show counter-rotation. The co-rotation of two sunspots has a simple explanation related to the emergence of a monolithic twisted flux tube. However, the reason for the counter-rotating sunspots requires further consideration. One possibility relates to the theory of Longcope and Welsch (2000), when the twists of the two polarities (footpoints of the assumed sunspot flux tube) are asymmetric. In this case, the twist would transfer from one polarity to the other through the connecting loop in the corona (see also Fan, Alexander, and Tian, 2009), eventually leading to opposite signs of the twist gradient normal to the solar surface, causing the appearance of counter-rotating sunspots (Y. Fan, private communication). Further study will help us to have better understanding of this scenario.

Acknowledgements The authors would like to thank Dr. Yuhong Fan for her valuable comments. The authors also thank SOHO/MDI for their data. SOHO is a joint project by ESA and NASA.

References

Brown, D.S., Nightingale, R.W., Alexander, D., Schrijver, C.J., Metcalf, T.R., Shine, R.A., Title, A.M., Wolfson, C.J.: 2003, Observations of rotating sunspots from trace. *Solar Phys.* **216**, 79 – 108.

Canfield, R.C., Hudson, H.S., McKenzie, D.E.: 1999, Sigmoidal morphology and eruptive solar activity. *Geophys. Res. Lett.* **26**, 627 – 630.

Chae, J., Jeong, H.: 2005, A method for determining magnetic helicity of solar active regions from SOHO/MDI magnetograms. *J. Korean Astron. Soc.* **38**, 295 – 298.

Chae, J., Wang, H., Qiu, J., Goode, P.R., Strous, L., Yun, H.: 2001, The formation of a prominence in active region NOAA 8668. I. SOHO/MDI observations of magnetic field evolution. *Astrophys. J.* **560**, 476 – 489.

Démoulin, P., Berger, M.A.: 2003, Magnetic energy and helicity fluxes at the photospheric level. *Solar Phys.* **215**, 203 – 215.

Evershed, J.: 1909, Radial movement in sun-spots. *Mon. Not. Roy. Astron. Soc.* **69**, 454 – 458.

Fan, Y.: 2009, The emergence of a twisted flux tube into the solar atmosphere: Sunspot rotations and the formation of a coronal flux rope. *Astrophys. J.* **697**, 1529 – 1542.
Fan, Y., Alexander, D., Tian, L.: 2009, On the origin of the asymmetric helicity injection in emerging active regions. *Astrophys. J.* **707**, 604 – 611.
Gibson, S.E., Fan, Y., Mandrini, C., Fisher, G., Demoulin, P.: 2004, Observational consequences of a magnetic flux rope emerging into the corona. *Astrophys. J.* **617**, 600 – 613.
Kazachenko, M.D., Canfield, R.C., Longcope, D.W., Qiu, J., DesJardins, A., Nightingale, R.W.: 2009, Sunspot rotation, flare energetics, and flux rope helicity: the eruptive flare on 2005 May 13. *Astrophys. J.* **704**, 1146 – 1158.
Liu, Y., Norton, A., Scherrer, P.: 2007, A note on saturation seen in the MDI/SOHO magnetograms. *Solar Phys.* **241**, 185 – 193.
Longcope, D., Welsch, B.: 2000, A model for the emergence of a twisted magnetic flux tube. *Astrophys. J.* **545**, 1089 – 1100.
Low, B.: 1996, Solar activity and the corona. *Solar Phys.* **167**, 217 – 265.
Magara, T., Longcope, D.W.: 2003, Injection of magnetic energy and magnetic helicity into the solar atmosphere by an emerging magnetic flux tube. *Astrophys. J.* **586**, 630 – 649.
Min, S., Chae, J.: 2009, The rotating sunspot in AR 10930. *Solar Phys.* **258**, 203 – 217.
Nightingale, R., Alexander, D., Brown, D., Metcalf, T.: 2001, Energization of rotating sunspots, twisted coronal fans, sigmoid structures, and coronal mass ejections. AGU, Fall Meeting, SH11C-0724.
Pevtsov, A.A.: 2002, Active-region filaments and X-ray sigmoids. *Solar Phys.* **207**, 111 – 123.
Rust, D., Kumar, A.: 1994, Helical magnetic fields in filaments. *Solar Phys.* **155**, 69 – 97.
Scherrer, P., Bogart, R., Bush, R., Hoeksema, J., Kosovichev, A., Schou, J., *et al.*: 1995, The Solar Oscillations Investigation – Michelson Doppler Imager. *Solar Phys.* **162**, 129 – 188.
Schuck, P.W.: 2006, Tracking magnetic footpoints with the magnetic induction equation. *Astrophys. J.* **646**, 1358 – 1391.
Solanki, S.K.: 2003, Sunspots: An overview. *Astron. Astrophys. Rev.* **11**, 153 – 286.
Tian, L.R., Alexander, D., Liu, Y., Yang, J.: 2005, Magnetic twist and writhe of delta active regions. *Solar Phys.* **229**, 63 – 77.
Welsch, B.T., Abbett, W.P., DeRosa, M.L., Fisher, G.H., Georgoulis, M.K., Kusano, K., Longcope, D.W., Ravindra, B., Schuck, P.W.: 2007, Tests and comparisons of velocity-inversion techniques. *Astrophys. J.* **670**, 1434 – 1452.
Yan, X.L., Qu, Z.Q., Xu, C.L.: 2008, A statistical study on rotating sunspots: polarities, rotation directions, and helicities. *Astrophys. J. Lett.* **682**, L65 – L68.
Zhang, Y., Liu, J., Zhang, H.: 2008, Relationship between rotating sunspots and flares. *Solar Phys.* **247**, 39 – 52.